DOI: 10.1002/smll.200700082

Carbon Nanotubes as Liquid Crystals

*Shanju Zhang and Satish Kumar**

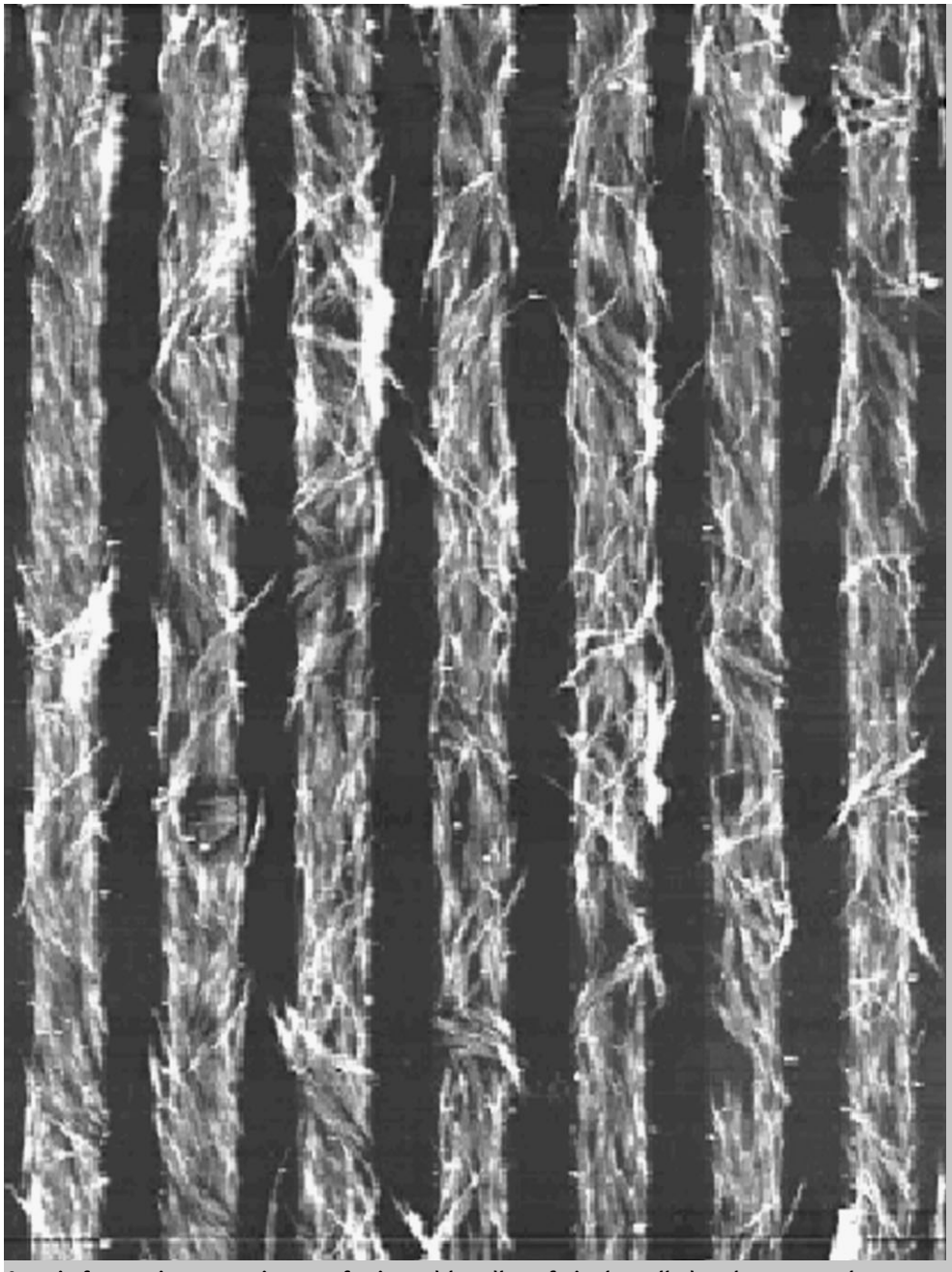

Atomic force microscopy image of oriented bundles of single-walled carbon nanotubes.

NANO MICRO small

From the Contents

Keywords:
- alignment
- carbon nanotubes
- liquid crystals
- phase behavior
- self-assembly

small NANO MICRO

Carbon nanotubes are the best of known materials with a combination of excellent mechanical, electronic, and thermal properties. To fully exploit individual nanotube properties for various applications, the grand challenge is to fabricate macroscopic ordered nanotube assemblies. Liquid-crystalline behavior of the nanotubes provides a unique opportunity toward reaching this challenge. In this Review, the recent developments in this area are critically reviewed by discussing the strategies for fabricating liquid-crystalline phases, addressing the solution properties of liquid-crystalline suspensions, and exploiting the practical techniques of liquid-crystal routes to prepare macroscopic nanotube fibers and films.

1. Introduction

Liquid crystal can be considered a fourth state of matter following solid, liquid, and gas. Liquid-crystal phases, as their name implies, exist between the conventional crystal phase and the liquid phase. Usually, liquid-crystal molecules possess rodlike or disclike anisotropic structures. The unique characteristic of liquid crystals is the tendency of the molecules to align themselves with long-range order. In general, rod-like liquid crystals exhibit nematic or smectic phases depending on the degree of the positional order (Figure 1). In the simplest form of nematic phase the molecules have only orientational but no positional order. The molecules are free to move but like to point along one particular direction, which is described by the director vector $\boldsymbol{n}$. The smectic phases are characterized by additional degrees of positional order and generally have separate layers within which there is a loss of positional order. The disclike liquid crystals normally form ordered columnar phases, which are characterized by stacked columns of molecules to form two-dimensional (2D) crystalline arrays (Figure 1).

In general, liquid crystals are most stable when all molecules are aligned along a single director. However, liquid-crystal molecules are highly sensitive to the external forces and thus, in most cases, liquid crystals contain defects, which are called topological disclinations.[1,2] The detailed molecular trajectories of a disclination are distinguished by strength s (the number of rotations in multiples of 2π of the director over a path encircling the disclination) and a value of constant parameter c in the simplest case, $\phi(\theta) = s\theta + c$, in which ϕ and θ are the director orientation angle and polar angle, respectively. According to Frank continuum theory,[3] one negative pattern and one positive pattern for $s = \pm\frac{1}{2}$, and one negative pattern and three positive patterns for $s = \pm 1$ can be expected in a 2D ordered liquid crystal (Figure 2). Knowing the disclination microstructure can shed light on defect mobility, which, in turn, affects the liquid-crystal properties, such as the alignment quality or rheological behavior.[4,5]

It has been suggested that carbon nanotubes (CNTs) are simply exceptionally stiff examples of rigid-rodlike macromolecules,[6] which due to their shape and size can act as liquid crystals. Liquid-crystal phases have been identified in the suspensions (or dispersions) of both multi-walled carbon nanotubes (MWNTs) and single-walled carbon nanotubes (SWNTs).[7–18] The ability of CNTs to form a liquid-crystal phase, its mesogenicity, depends predominately on its straightness and its aspect ratio. Liquid-crystal structures in the CNT suspension can be maintained in the solid film when the solvent is completely evaporated. The individual CNT orientation around the disclination and the central core can be directly visualized under high-resolution scanning electron microscopy (HRSEM)[7,8] or atomic forcing microscopy (AFM)[13]. Therefore, the liquid-crystal system of CNTs serves as a model for studying physical issues of considerable interest in liquid-crystal science.

Kevlar, a rigid-rod polymer of poly(*p*-phenylene terephthalamide) (PPTA), is an example of commercially successful liquid-crystalline polymers. Kevlar exhibits so-called lyotropic liquid crystallinity in solution as a function of polymer concentration.[19] Carbon nanotubes, analogous to Kevlar, also exhibit lyotropic liquid crystallinity in a suspension under certain conditions.[7–18] This analogy is applicable to fabricating macroscopic films and fibers of CNTs by using the liquid-crystal phase to achieve high alignments within the films and fibers.[20–22] The SWNT fibers spun from a liquid-crystalline phase in a super acid had a misalignment of $\pm 15.5^\circ$ and a Young's modulus of about 120 ± 10 GPa,[20] while MWNT fibers spun from a liquid-crystal phase in ethylene glycol had a misalignment of only $\pm 7.8^\circ$ and a Young's modulus of 142 ± 70 GPa.[21] These modulus values of CNT fibers are comparable to those of Kevlar fiber. However, a large amount of further work will have to be done before commercialization of CNT fibers by liquid-crystal spinning.

In this Review, we give a critical overview of literature reports of CNTs exhibiting liquid crystallinity and their applications. We briefly discuss rigid-rod liquid-crystalline theories of CNT systems in Section 2 and strategies for fabricating liquid-crystalline phases of CNTs are discussed in Section 3. In Section 4, we present solution properties of CNTs in liquid-crystalline phases. Next, we address technical

[*] Dr. S. Zhang, Prof. S. Kumar
School of Polymer, Textile and Fiber Engineering
Georgia Institute of Technology
Atlanata, GA 30332-0295 (USA)
E-mail: satish.kumar@ptfe.gatech.edu

developments using liquid-crystal routes for CNT fiber and film formation. Finally, we give a summary and outlook.

2. Liquid-Crystal Theory of Carbon Nanotubes

The liquid-crystal nature of CNTs can be understood using the steric theory of rigid-rodlike liquid crystals.[23,24] Based on the simple steric model, no two molecules occupy the same space and the molecular configurations are dominated by steric repulsive interactions. The model describes the equilibrium phase diagram depending on the concentration. Both translational and rotational degrees of freedom contribute to the entropy of the system at a given concentration. In a dilute solution, the translational entropy dominates over the rotational entropy because of the large free volume. Therefore, the parallel configuration of molecules is not favored and the phase is isotropic. While in a concentrate solution, reducing the free volume increases parallel configurations to optimize the packing efficiency. The rotational entropy is thereafter predominant, leading to the liquid-crystalline phase. In reality, many factors such as particle–particle interaction, particle–solvent interaction as well as the tortuosity and polydispersity of the particles play a role in controlling the phase transition.[25]

CNTs are a very complex system. From a theoretical viewpoint, CNTs can be considered as model straight, long, rigid-rodlike particles. The steric theory for the electrostatic repulsion of long rigid rods has been used to investigate the SWNT phase behavior in their suspension.[26] Calculations have shown that SWNTs in a good solvent is analogous to the classic rigid-rod system if the van der Waals force between CNTs is overcome by strong repulsive intertube potentials. The nematic phase starts to form at a volume fraction of about $3.3\,d/l$ and fully develops at about $4.5\,d/l$, where d and l are tube diameter and tube length, respectively.[26] When the solvent is not good for SWNTs, the van der Waals attractive interactions between the nanotubes are still strong. As a result, only extremely dilute solutions of SWNTs are thermodynamically stable and no liquid-crystal phases form at room temperature.

Considering the effect of temperature on the phase behavior, the liquid crystallinity of finite-size capped CNTs with and without full van der Waals interactions has been analyzed by using continuum-based density-functional theory.[27] The resultant phase diagram is complex, which describes temperature (T) versus concentration (η) for CNTs with different aspect ratios (Figure 3). In the presence of full van der Waals interactions, the nematic phase as well as columnar phase occur in a wide range of very high temperatures. The existence of the columnar phase is very interesting, as the ordered columnar phase normally occurs in the disclike liquid crystals.[28] The columnar phase predicted by theory is assumed to be analogous to the hexagonal ordering of SWNTs in the rope, which is commonly observed in high-temperature-synthesized SWNTs.[29] Although such an analogy remains questionable, the predominant columnar phase at high temperature predicted by theory can explain the stability of the SWNT ropes during their growth at high temperature in extreme conditions. In the absence of van der Waals interactions, the system is dominated by steric repulsive interactions only. With an increase of concentration, the system undergoes an isotropic-to-nematic phase transition via a biphasic region, the so-called Flory chimney in the liquid-crystalline polymers.[25] The longer the CNTs, the lower the concentration needed. The ordered smectic phase is predicted at higher concentration over $\eta \sim 0.36$. This calculation is consistent with that of simple rodlike liquid crystals.

The above theoretical calculations have shown that to form liquid-crystal phases at room temperature, strong van der Waals attractions between CNTs must be screened out. This requires a good solvent with an ability to disperse CNTs down

Shanju Zhang received his B.Sc. in chemistry from Jilin University (P.R. China) in 1993 and his Ph.D. in polymer chemistry and physics from the same university in 1998. From 1998 to 2000 he was an assistant professor at Changchun Institute of Applied Chemistry at the Chinese Academy of Sciences. In 2000, he moved to the Johannes Gutenberg University of Mainz (Germany) and later worked at the Technical University of Berlin (Germany) as a postdoctoral fellow. He received an Alexander von Humboldt fellowship in Berlin in 2000. From 2002 to 2006 he worked in the Cavendish laboratory and Materials Science department at the University of Cambridge (England) as a research associate. Since 2006, he has been a research scientist in the school of Polymer, Textile and Fiber Engineering at Georgia Institute of Technology (U.S.A.). His research interest is in the area of soft matter, including liquid crystals, polymers, carbon nanotubes, and biomaterials.

Satish Kumar received his Ph.D. degree in 1979 from the Textile Technology Department at the Indian Institute of Technology, New Delhi, India in the area of polymer and fiber science. He obtained his postdoctoral experience in the Polymer Science and Engineering department at the University of Massachusetts (1979–82). During 1982–83, he was a visiting scientist at the Atomic Energy Commission of France, C.E.N.G., Grenoble, France. During 1984–89 he was associated with the Polymer Branch, Air Force Materials Laboratory, Wright Patterson Air Force Base, Dayton, OH on contract through Universal Energy Systems and the University of Dayton Research Institute. He joined the faculty of the School of Polymer, Textile and Fiber Engineering at Georgia Tech in 1989, where he is currently serving as a Professor. Dr. Kumar has published extensively in the areas of structure, processing, and properties of polymers and fibers. His current research is focused on polymer–carbon-nanotube composites.

NANO MICRO small

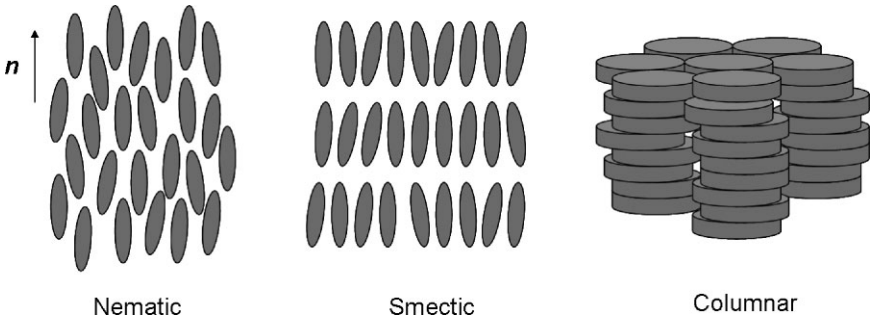

Figure 1. Schematic image of liquid-crystal structures in nematic, smectic, and columnar phases.

to the level of individual tubes. Experimentally, several strategies have been successfully developed to increase repulsive interactions between CNTs or to concentrate them by gradually evaporating the solvent or to form aligned phases by flowing the CNTs. These include negative or positive charging of CNT surfaces,[7–10] polymer wrapping,[15,16] drop drying,[12–14] and shear flow.[17] In the following section, we will discuss in detail how each approach works to create liquid-crystal phases in CNTs.

3. Fabrication of Liquid-Crystalline Phases

3.1. Acid Oxidation

Acid oxidation is an efficient approach to modify the CNT surface by introducing functional groups.[30] Typically, CNTs are treated by using a mixture of concentrated sulfuric acid and concentrated nitric acid (H_2SO_4/HNO_3) at a 3:1 ratio in volume under ultrasonication. After treatment, the CNTs are not only cut into short tubes but also functionalized by carboxylic, carbonyl, and hydroxyl groups. The presence of oxygenated groups on CNTs negatively charges the CNT surface and thereafter enhances the dispersibility and stability of the CNTs in a polar solvent without any additives. In this case, the intertube van der Waals interactions are overcome by electrostatic repulsion and CNTs are thus analogous to charged rigid-rodlike particles. The reported concentration value of acid-oxidized CNTs in water is up to 8 wt%.[8]

While much effort has been made to address CNT dispersibility and surface chemical functionalization via acid oxidation,[31–33] little attention has been paid to the phase behavior of acid-oxidized CNTs. In 2003, Windle's group first reported the liquid-crystalline behavior of an aqueous suspension of acid-oxidized MWNTs[7] and analyzed the phase diagram using the simple rigid-rod steric theory.[8] The liquid-crystalline behavior of CNTs has now been reported in several systems.[9–18]

In a dilute aqueous solution, the acid-oxidized CNTs behave as Browian particles, forming an isotropic phase.[7,8] With an increase in concentration above the percolation threshold, the nematic nuclei due to steric effects grow and coagulate into large nematic domains. The liquid-crystalline domains coexist with isotropic regions, which remain dark irrespective of the rotation setting of the crossed polars. This shows a biphasic suspension in equilibrium, which is analogous to the Flory chimney in the rigid-rodlike liquid crystals.[25] Further increasing the concentration leads to a single liquid-crystal phase. The whole phase transition for aqueous suspension of MWNTs under polarized optical microscope is shown in Figure 4. The observed Schlieren texture is a

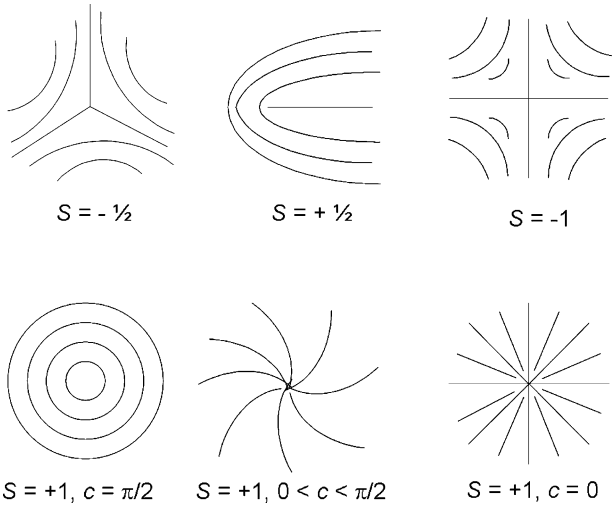

Figure 2. Molecular trajectories in a 2D ordered liquid crystal associated with disclinations of $s = \pm\frac{1}{2}$ and ± 1.

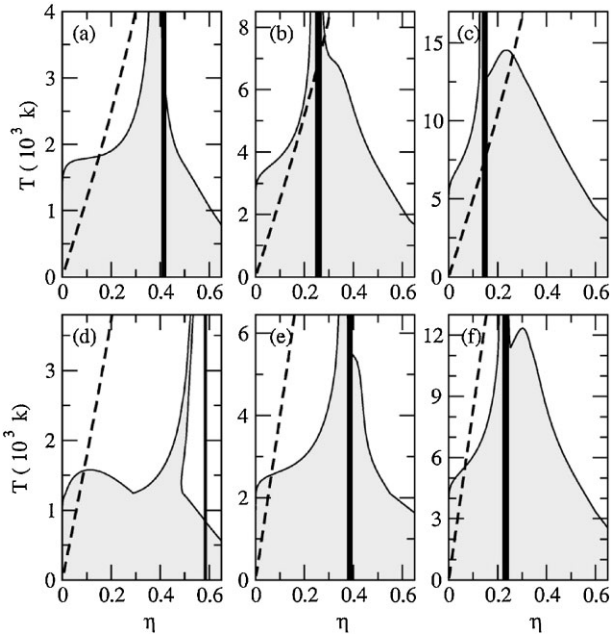

Figure 3. Theoretically calculated phase diagrams for carbon nanotubes with different aspect ratio as a function of temperature T and fraction η: a) 70, b) 140, c) 280, d) 37, e) 74, and f) 148. The shaded gray region denotes the isotropic–nematic coexistence region and the dashed line the nematic–columnar spinodal. The thick line marks the isotropic–nematic coexistence region in the absence of van der Waals force. Reprinted with permission from Reference [27]. Copyright 2001, American Physical Society.

typical optical effect of nematic liquid crystals. This phase behavior of MWNTs is consistent with the theoretical predictions in the simple rigid-rod particles[23,24] as well as in the CNT systems.[26,27]

The critical concentrations for starting the nematic phase (c^1*) and ending the isotropic phase (c^2*) depend on the solvent quality and aspect ratio of the CNTs.[8] In the case of MWNTs with an aspect ratio of 30, the reported critical concentrations c^1* and c^2* are 1.0 vol % and 4.0 vol %, respectively,[8] while the simple rigid-rod theory predicts that a biphase for monodisperse liquid crystals is typically at a ≈1–2 vol % concentration range depending on the aspect ratio.[25] The comparatively large range of the Flory chimney is assumed to associate with polydispersity in terms of length, diameter, and straightness of the CNTs. The widening effect of the Flory chimney due to size polydispersity has been recognized in polymeric liquid crystals before.[34,35] Reducing polydispersity of polymer chains significantly narrows the Flory chimney toward reaching the theoretical prediction. Recently, the liquid-crystal phase diagram of aqueous suspension of monodisperse MWNTs has been investigated.[36] Acid-oxidized CNTs can be fractionalized and purified in the biphasic regions by centrifugation.[36] Long nanotubes enter the liquid-crystalline phase, which can be removed and refractionized by adding more solvent. With an increase of centrifugation cycles, the CNT length range becomes smaller and the Flory chimney becomes narrower. This method is very efficient to size fractionize nanotubes based on their liquid crystallinity and therefore allows the polydispersity to be greatly decreased. The values of c^1* and c^2* for monodisperse MWNTs with a length of 900 nm and a diameter of 30 nm are reported to be about 1.6 wt% and 4.5 wt%, respectively.[36] The ratio of c^2*/c^1* is about 2.8, which is in agreement with the theoretical value of ≈2–3 for a system of rigid rods with the most probable distribution.

The liquid-crystalline structures including the singularities of the Schlieren texture can be preserved as a thin film after the solvent is completely evaporated from the suspension.[7,8,36] This preservation provides further opportunity to study disclination supramolecular microstructures using SEM or AFM at a resolution sufficient to view individual CNTs. In particular, it is possible to visualize the individual CNT contribution to distortions of the director field and central core of the disclination. For a polydisperse system of liquid-crystalline polymers, it has long been speculated that short polymer chains have a tendency to aggregate in the disclination cores, where they reduce the high elastic-distortion energies.[37,38] CNT liquid crystals have the ability to directly visualize such segregation in the polydisperse system,[36] in which short tubes and impurities are in the central core (Figure 5). After CNT size fractionation, the disclination cores decrease and no segregation of short tubes or impurities appears in the core (Figure 5).

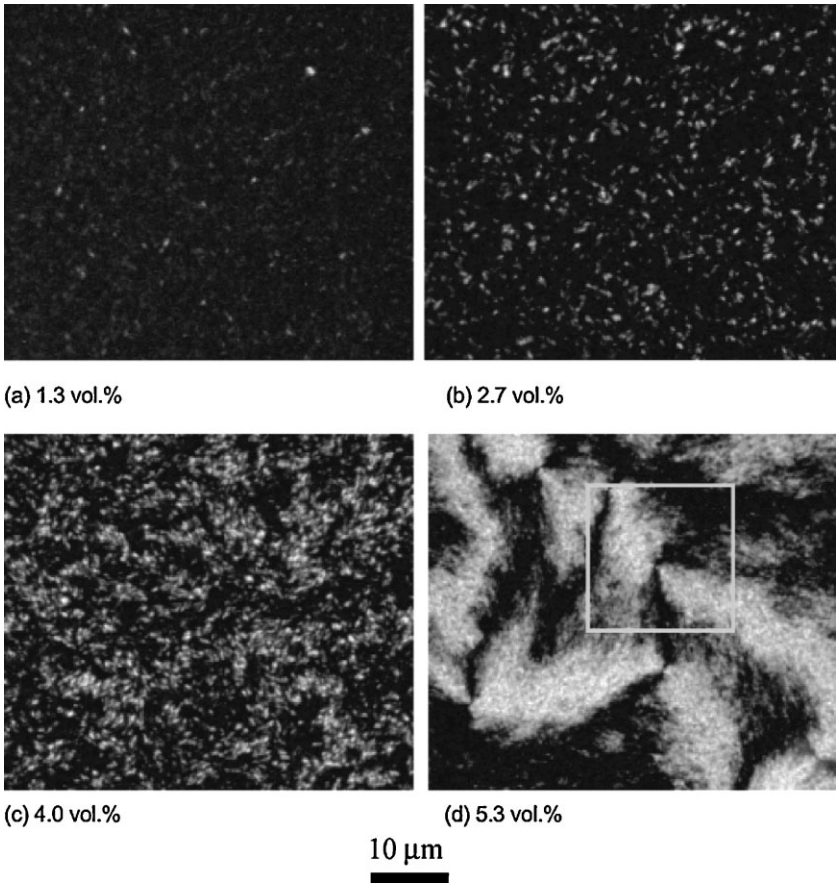

Figure 4. Optical images of MWNT aqueous suspensions with crossed polarizers showing the phase transition from isotropic to the liquid-crystal phase with increasing concentration. Reprinted with permission from Reference [8]. Copyright 2005, American Chemistry Society.

3.2. Acid Protonation

It has been suggested that CNTs can behave as a weak base and be protonated by superacids.[9,10] As a result, the delocalization of positive charge over the entire CNT occurs. Such protonation yields the formation of ordered acid layers on the CNT surfaces and thus the dissolution of CNTs.[39,40] Based on X-ray data,[39,40] a three-layer model has been suggested (Figure 6). The acids in the innermost layer have positional and orientational molecular order, showing strong association between CNTs and superacids. In the middle layer, acid molecules interact with the innermost layer via hydrogen bonding, forming semiordered regions. In the outermost layer, acid molecules behave as bulk disordered regions.

The ordered acid layers around CNTs produce intertube electrostatic repulsions, which are strong enough to overcome the intertube van de Waals attractions. It has been reported that the SWNTs can be dispersed in superacids, such as 100% sulfuric acid, oleum (20% free SO_3),

small NANO MICRO

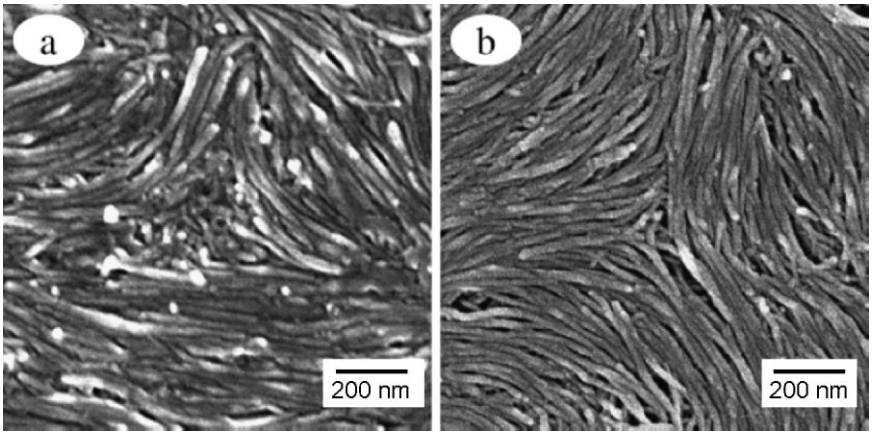

Figure 5. SEM images of a $-\frac{1}{2}$ disclination in the nematic phase of MWNTs: a) unpurified materials and b) purified materials. Reprinted with permission from Reference [36]. Copyright 2006, American Chemistry Society.

triflurometha nesulfonic acid (triflic acid), methanesulfonic acid, and chlorosulfonic acid, with a concentration of up to 8 wt%.[41] Again, the protonated SWNTs in the superacid behave as rigid-rodlike liquid crystals and exhibit an isotropic-to-nematic phase transition with an increase in concentration over a critical value.[9,10] The phase diagram of SWNTs in superacids is reminiscent of those in the lyotropic rigid-rod polymers and particles.

As in the rigid-rodlike liquid crystals, solvent quality greatly affects the SWNT–solvent interaction and thereafter the phase diagram of the system investigated. It has been reported that the critical concentration of the isotropic-to-nematic transition for SWNTs in superacids shifts towards a higher value with an increase of acid strength.[10] Thus, the isotropic phase of SWNTs in superacids becomes more stable when the acid strength is high. Stronger acids have greater protonating power, resulting in increased charge stabilization and the overall number of SWNTs in the isotropic phase. These findings further confirm the protonation mechanism of CNTs in superacids. From a viewpoint of the stabilization of CNT suspension, this system also opens a new route to improve the dispersibility of CNT suspension.

Acid oxidation and acid protonation are very efficient methods to introduce negative or positive charges on the CNT surface to create electrostatic repulsions. This intertube electrostatic interaction can overcome the intertube van der Waals attraction. The resultant CNTs are exfoliated and they behave as rigid-rodlike liquid crystals.

3.3. Polymer Wrapping

Polymer-wrapped CNTs can be effectively dispersed in a solvent without damaging CNTs. Polymers used to increase CNT dispersibility include conjugated polymers,[42] amphiphilic block copolymers,[43] polyelectrolytes,[44] and biopolymers.[45] Depending on the polymer structures and polymer–CNT interactions, the polymer-wrapped CNTs can be dispersed and stabilized in a solvent with a considerable concentration. With an increase of suspension concentration, the suspensions of polymer-wrapped CNTs undergo an isotropic-to-nematic phase transition under certain conditions.[15,16,46]

In an aqueous medium of a water-soluble polymer, the hydrophobic CNT surface can be eliminated by polymer wrapping around the CNTs. Biopolymers such as DNA and polysaccharides have been used to wrap SWNTs and to increase tube dispersibility in water.[15,45] DNA is a charged amphiphilic polymer that can be strongly adsorbed on the CNTs. The electrostatic repulsions between DNA molecules can overcome the intertube van der Waals attractions and therefore DNA can effectively disperse CNTs in water. As in the case of acid-treated CNTs, the phase diagram of DNA-wrapped SWNTs is similar to those of lyotropic rigid-rod polymers.[15,16] There is a biphasic region (2–4 wt%) before the system enters a single-liquid-crystal phase (Figure 7). The liquid-crystalline behavior of SWNTs with such biological molecules is particularly interesting. Liquid-crystal phases have been frequently observed for biologically important molecules including lipids, nucleic acids, carbohydrates, and proteins in vivo as well as in vitro under well-controlled conditions.[47] Moreover, liquid-crystal ordering may be relevant to the biological function and self-assembly processes associated with each biological molecule. Recent work on liquid-crystal materials used in the biosensors and medicines has shown promise for the new revolution of liquid crystals in biological systems.[48,49]

Polymer wrapping provides a direct way to create intertube repulsive interactions to overcome van der Waals attractions. As a result, the concentration of the CNT dispersion, in some special conditions such as strong binding interactions between CNTs and polymers, is high enough to allow the system to enter a nematic liquid-crystal phase. However, the CNT–polymer interactions in most cases are not strong enough to stabilize the suspension at a significant concentration by such physical wrapping. Approaches to create a spontaneous phase transition from the isotropic to the liquid-crystal phase in CNT systems are highly desired.

3.4. Gradual Evaporation

Drop drying has been widely used for fabricating 2D ordered structures of nanoparticles.[50] Drops of the solvent are put on the solid substrate surface and are allowed to evaporate by controlling the drying rate. As the solvent evaporates, the liquid level sweeps over the substrate, depositing the solute behind as an ordered assembly when the solvent is completely gone. This gradual evaporation process starting from the dilute solution has been used for organic rigid-chain polymers,[51] inorganic nanorods,[52] and DNA[53] to create liquid-crystalline assemblies on the substrate. The convective flow due to the solvent evaporation carries the rodlike objects from the bulk solution to the liquid–solid–

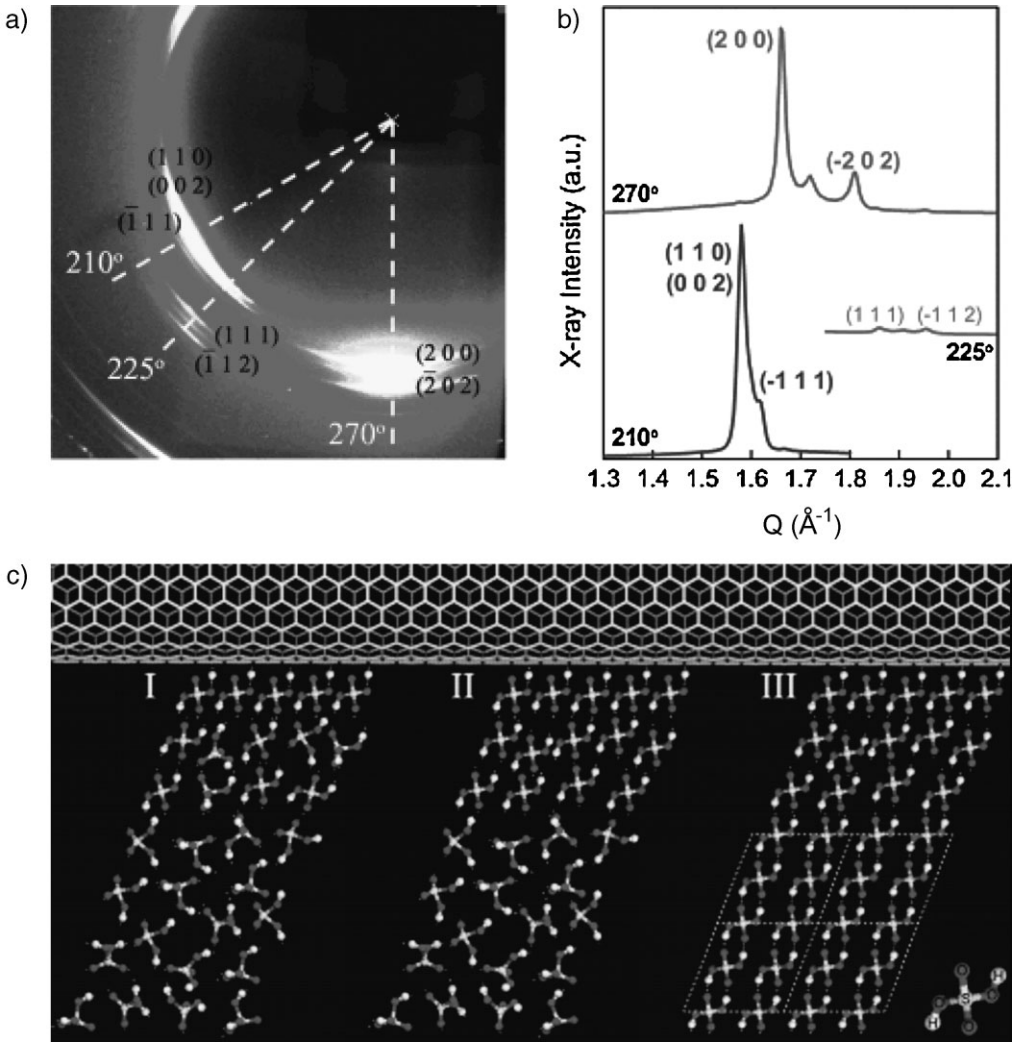

Figure 6. X-ray diffraction patterns of a SWNT fiber with excess free sulfuric acid at 200 K showing the ordered orientation of acid crystallites (top) and schematic image showing crystallization of acids templated by SWNTs (bottom). I, II, and III represent the liquid phase, the semiordered region, and the crystallization of acids, respectively. Reprinted with permission from Reference [39]. Copyright 2006, American Chemistry Society.

air interface and can make the solution locally very concentrated; the phase transition from isotropic to liquid-crystal can therefore occur. Such an evaporation-induced liquid-crystal phase transition from an isotropic phase and subsequent self-assembling on the substrate have been recently reported for CNT systems.[12,13]

It has been recognized that surfactant wrapping is a very popular method to disperse CNTs in aqueous medium due to their commercial availability. However, the surfactant-wrapped CNT systems typically have a very low concentration and the systems are isotropic.[54] By using the drop-drying process, the phase transition from isotropic to nematic phase has been observed in the aqueous suspension of sodium dodecyl sulfate (SDS)-coated SWNTs.[12,13] After complete water evaporation, the SWNT thin films show very high CNT alignment and the intensity ratio of radial breathing mode (RBM) peaks of SWNTs in the Raman spectrum for polarization parallel and perpendicular is 20:1.[55] It has been found that substrates such as a clean Si wafer, transparent glass slide, and plastic film have little effect on the SWNT liquid-crystal formation.[12] However, factors such as suspension concentration and temperature have a significant effect on the liquid-crystal formation and CNT alignment. Lower concentration and higher evaporation temperature can enhance the liquid-crystal ordering, as the liquid-crystal defects interact with each other toward single domain structures.

An alternative method to create CNT liquid crystals is to gradually evaporate the solvent to reach a nematic transition by embedding CNTs in an isotropic gel.[56,57] The isotropic gel can be prepared by polymerizing the aqueous mixture of SDS-coated SWNTs and a crosslinkable monomer, for example, isopropyl acrylamide. The resulting gel has a SWNT concentration of 0.3 wt %, in which SWNTs are homogenously and randomly distributed. The isotropic SWNT gel is then heated at an elevated temperature to expel the solvent, which produces a large compression volume change. During the gel shrinking, the SWNT concentration increases without apparent CNT aggregation. When the SWNT concentration in the gel increases above a critical value such as 2.4 wt%, the SWNT gel exhibits strong birefringence, indicating the formation of a

NANO MICRO small

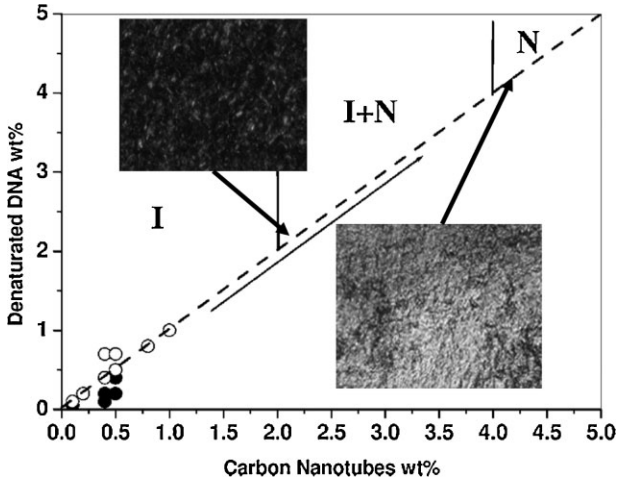

Figure 7. Phase diagram of DNA-wrapped SWNTs in water. The dashed line shows the limit above which SWNTs are homogeneously dispersed after sonication (white circles); below the line, aggregations are still observed (black circles). Insets: optical images with cross polarizers in biphasic and nematic phases. Adapted from Reference [15].

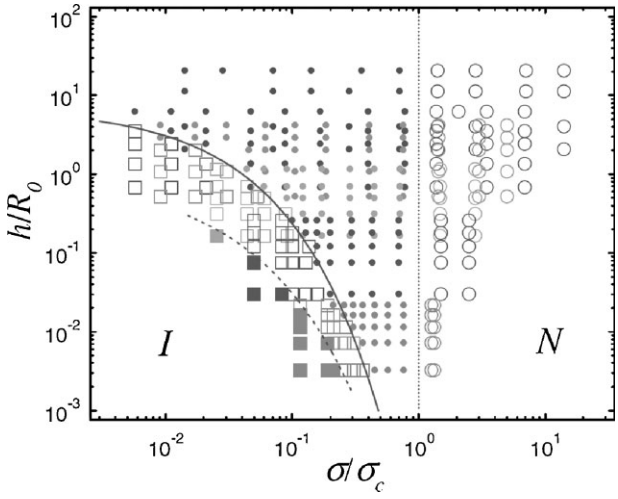

Figure 8. Phase diagram of long CNTs suspended in a polymer liquid under shear flow. The concentration increases from top to bottom. Dashed lines mark the stability limit. Open circles are nematics, closed circles are isolated aggregates, open squares are vorticity bands, and closed squares are cavitated networks. N and I present nematic and isotropic phases, respectively. Reprinted with permission from Reference [17]. Copyright 2006, American Physical Society.

nematic phase. It is interesting to note that the critical concentration from isotropic to nematic phase in the gel is close to those in other systems described above. This result indicates that the isotropic-to-nematic phase transition of SWNTs in the gel is still dominated by the rotational entropy as those of unconstrained Brownian particles in the solution.

3.5. Shear Flow

While the above-discussed short CNTs (typically less than 1 μm) are extremely stiff and exhibit liquid-crystalline behavior with increasing concentration over a critical value in the suspension, the long CNTs are soft and typically due to entanglements form disordered networks in equilibrium.[58,59] Considering the real values for application of the long CNTs, creating liquid-crystal phases in the long-CNT suspension is more meaningful.

It is well known that shear flow can induce liquid-crystal ordering of the long-chain macromolecules in their suspension.[60,61] The shear forces could induce the polymer flow and orient along the shear direction, resulting in an isotropic-to-nematic phase transition. Following the similar physical principle, shear-induced nematic phases of long-CNT suspension have been reported.[17,63] It is found that a critical mixing time t^* is needed to achieve a homogeneous dispersion, which is dependent on the long-CNT concentration and on the shear stress.[62] With an increase in concentration, shear stress and aspect ratio, the nematic ordering of long CNTs significantly increases. A universal liquid-crystal phase diagram of long CNTs with an aspect ratio of 200 has been developed,[17,63] which describes a first-order phase transition from isotropic disordered networks to (para)nematic liquid crystals under the shear field (Figure 8). While the long CNTs are strongly non-Brownian, their phase behavior under the shear field is found to be similar to those of rigid-rodlike particles. Better understanding of phase transitions of the long-CNT suspension under the shear field is required in order to control their alignment during processing.

The fact that shear induces the nematic phase in long CNTs is very valuable from a practical viewpoint. It provides a way to control CNT alignment during processing, while maintaining their unique electronic and mechanical properties.

4. Solution Properties in Liquid-Crystalline Phases

4.1. Rheology

The rheology of CNT liquid-crystal suspensions is similar to those of rigid-rodlike liquid-crystalline polymers. Figure 9 shows the rheological behavior of SWNTs in superacids.[9] The viscosity-versus-concentration curve is not monotonic, where the viscosity first reaches a maximum value with an increase in concentration and then falls to a minimum value in a single nematic phase. Increasing the shear rate results in lower viscosity, indicating a shear-thinning effect. The first normal stress difference N_1 due to the orientation of CNTs by flow is the first-order elastic effect, showing negative values. The negative N_1 indicates compression along the streamlines and tension in the cross-stream direction.

It is well recognized that the polymer solution or melt swells due to the positive N_1 when it is extruded from the die.[64] This die swell results in an irregular extruded shape and affects the physical properties of the resulting products. The negative N_1 in the CNT liquid-crystal dispersions is very meaningful for practical technique developments, as it could be exploited to eliminate the die swell.[65] Further work to investigate the origin of the negative N_1 and to develop industrial techniques for the exploitation of the negative N_1 effect for improving the CNT-based materials properties are desirable.

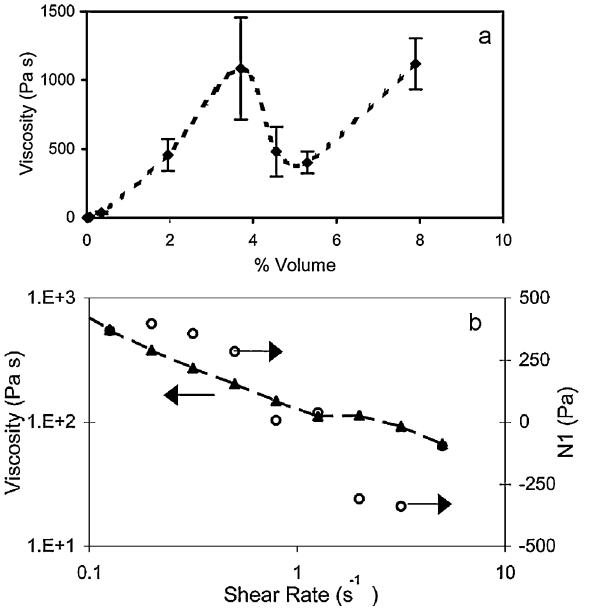

Figure 9. a) Viscosity versus concentration for SWNTs in superacids at a shear rate of 0.1 s^{-1} and b) viscosity versus shear rate for 4.5 vol% SWNTs in superacids. N_1 is the thrust on the plate divided by the plate area. Reprinted with permission from Reference [9]. Copyright 2004, American Chemistry Society.

4.2. Phase Separation

One of the unique characteristics in lyotropic rigid-rod polymers is the biphasic region in equilibrium where the isotropic and liquid-crystalline phases coexist.[25] In the polydisperse system, liquid-crystal forming ability (mesogenicity) of polymer chains is dependent on their length and straightness. The polymeric molecules with lengths below their persistence length diffuse preferentially to the disordered isotropic phase. As a result, the macroscopic phase separation with size fractionation occurs within the Flory chimney in equilibrium. Such phase separations have been well recognized in the solutions of classical rigid-rod liquid-crystalline polymers.[66,67]

Similar to the lyotropic rigid-rod polymers, the CNT liquid-crystal suspension also exhibits a biphasic region and can phase separate into nematic domains in equilibrium with an isotropic phase over time.[8–10,36] The time required for phase separation to occur is dependent on the CNT length and concentration. Macroscopic phase separation in the Flory chimney can be obtained on centrifuging the biphasic suspension or allowing it to stand.[36] After phase separation by centrifugation, two layers are identified in the centrifugation tube with an isotropic phase in the top layer and a nematic phase in the bottom layer. Long and straight CNTs with higher mesogenicity segregate preferentially to the nematic phase in the bottom layer, whereas shorter CNTs and impurities with lower mesogenicity segregate preferentially to the isotropic phase in the top layer (Figure 10a and b). This is confirmed by SEM imaging (Figure 10c and d). Furthermore, such interphase fractionation can be repeated as a purification method by an iterative process. As a result, the Flory chimney decreases in width with each successive cycle of centrifugation,

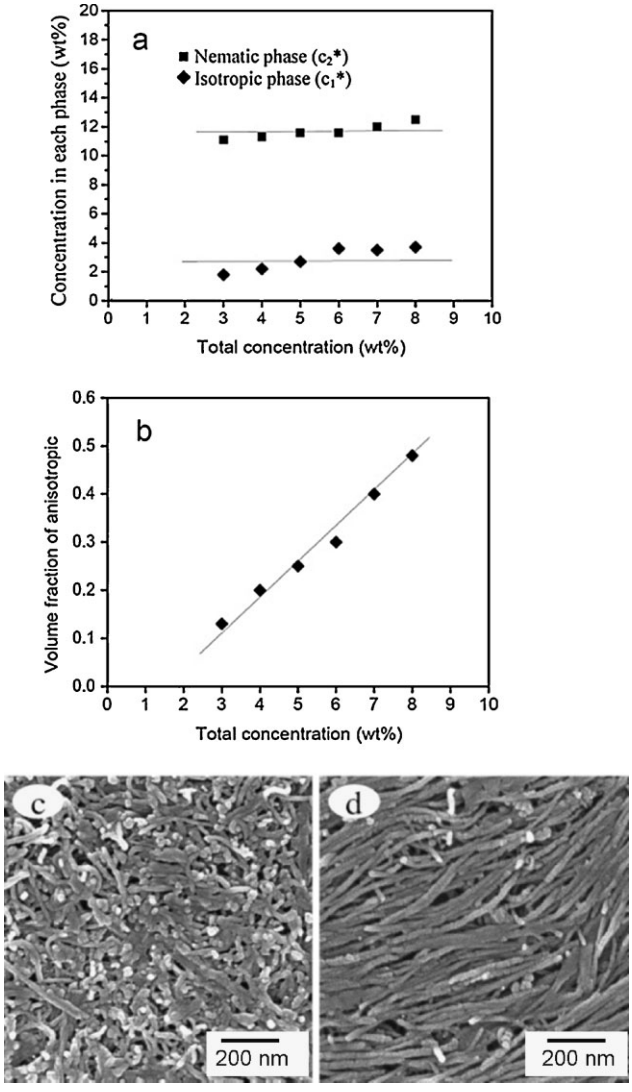

Figure 10. Plots showing a) volume fraction of MWNTs in each of the phases coexisting in the Flory chimney as a function of overall concentration after centrifuging the sample, b) the volume fraction of the nematic phase over the same range of total concentration, and SEM images of c) isotropic and d) nematic phases. Reprinted with permission from Reference [36]. Copyright 2006, American Chemistry Society.

indicating narrower CNT length distribution. The process provides a promising route to a way of sorting CNTs by their length upon separation of the nematic and isotropic phases. This method would be very useful for the analysis and purification of CNTs to produce monodisperse samples, which would be of significant scientific and technological value.

Phase separation can also occur in long-CNT suspensions under shear flow.[68] With increasing shear rate, longer flow-aligned CNTs move into the bulk, whereas shorter CNTs move onto the shearing surfaces. In addition to the mesogenicity of CNTs, the geometrical confinement may play an important role in such length-fractionation phenomenon.

4.3. Optical Anisotropy

The optical anisotropy of liquid crystals yields a birefringence. Typical Schlieren textures of a nematic phase have been

NANO MICRO small

reported in liquid-crystal phases of the CNT suspensions.[7–18] The anisotropy of optical absorption can be obtained by measuring the transmission intensities of plane-polarized light through birefringent domains with polarization parallel and perpendicular to the CNT alignment axis. Birefringence of the CNT suspension at a critical value of concentration abruptly increases with a change of order parameter, S, from 0.3 to 0.8, indicating a first-order transition of isotropic-to-nematic phases.[56] Under the shearing field, the optical anisotropy of CNT suspensions strongly depends on the shear rate and CNT concentration.[68] Increasing shear rate and CNT concentration results in increased birefringence, similar to those of liquid-crystalline polymers.

5. Liquid-Crystal Processing of Macroscopic Assemblies

The demonstration of liquid crystallinity in the CNT suspensions has opened up a rich field of study, not only as a new system of interest to liquid-crystalline science but also as a basis for a range of technological developments in the processing of CNTs into useful material forms such as fibers and thin films. Well-aligned macroscopic assemblies represent a practical development in the exploitation of liquid crystallinity in CNT technology using routes analogous to those developed for commercial rigid-rodlike liquid-crystalline polymers.

5.1. CNT Fibers

A number of approaches to spin neat CNT fibers without the use of polymers have been reported. These include gas-phase spinning from a chemical vapor deposition (CVD) reactor,[69–72] solid-state spinning from vertically aligned CNT arrays,[73–77] and coagulation wet-spinning from the liquid-crystalline phase.[20–22] Liquid-crystal spinning is promising as this process has the potential to produce very high CNT orientation, which is crucial for obtaining high-modulus fibers.

In liquid-crystal spinning, the CNT liquid-crystal suspension is extruded through a capillary spinneret into a coagulation bath that contains a second liquid in which the CNT solvent is soluble but the CNTs themselves are not. The CNTs therefore phase separate and condense to form a fiber. As the shear forces orient liquid-crystal domains of CNT suspension during the extrusion process, the resulting CNT fibers are highly oriented.

SWNT fibers have been successfully spun from their liquid-crystalline phase in sulfuric acid[20] using the wet-spinning technique similar to those of liquid-crystalline polymer fibers (Figure 11). The G-band Raman ratio for polarization parallel and perpendicular to the SWNT fiber axis is 20:1 and the SWNT misalignment is $\pm 15.5^{\circ}$. This alignment was obtained without any post-drawing process, indicating that the liquid-crystalline nature of the SWNT suspension is mainly responsible for this orientation. The reported Young's modulus of the SWNT fibers is 120 ± 10 GPa, similar to that of the Kevlar-49 fiber. The internal microstructures of SWNT fibers show a substructure of superropes of $\approx$200–500 nm in diameter throughout the fibers.[20] These superropes in SWNT fibers are analogous to the elemental microfibrils commonly observed in rodlike liquid-crystalline polymer fibers.[25]

MWNT fibers have also been fabricated from their liquid-crystalline phase in ethylene glycol.[21] The CNT misalignment in the MWNT fibers varied from $\pm 7.8^{\circ}$ to $\pm 10.1^{\circ}$ depending on the CNT straightness. With an increase in CNT alignment, the modulus of the MWNT fibers increased and the best value is reported to be about 142 ± 70 GPa. These results fit into known polymer-fiber theory, where mechanical properties of the fiber increase with the polymer orientation.[78] The 1-mm-long MWNTs have been spun into the fibers using this

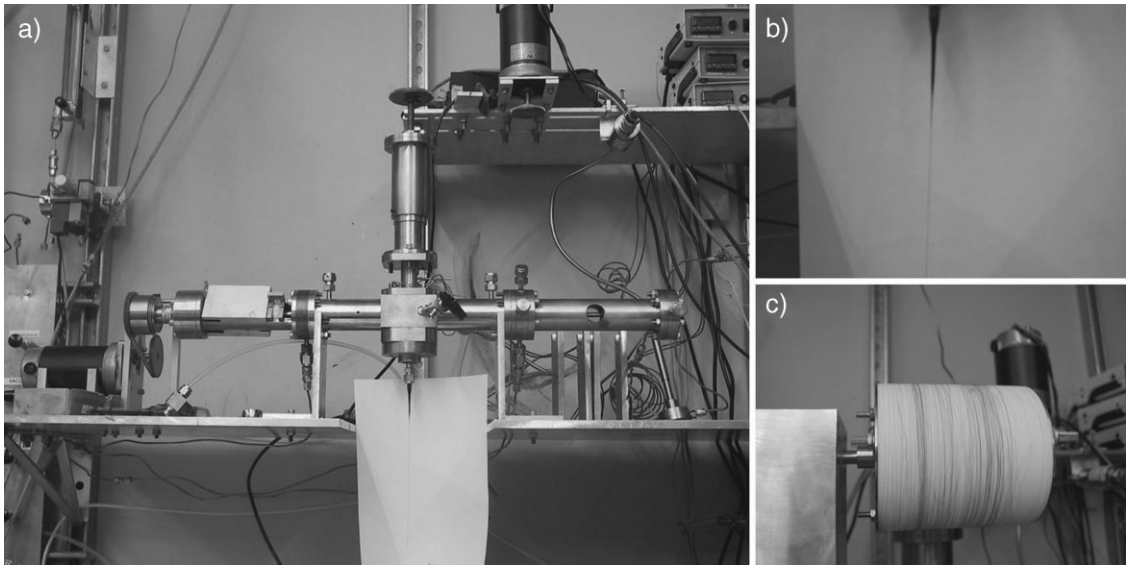

Figure 11. Solution-spinning process for SWNT fibers from liquid-crystalline phase in sulfuric acids: a) apparatus used for extruding fibers, b) a jet of SWNT dispersion being extruded from the capillary spinneret, and c) a 30-m-long example of SWNT fibers. Reprinted with permission from Reference [20]. Copyright 2008, AAAS.

method.[22] Longer nanotubes are expected to increase the intertube contact area and hence the tensile strength of the resulting fibers.

As in liquid-crystal spinning of polymeric fibers, the microstructure and physical properties of the CNT fibers are largely dependent on the spinning conditions, coagulation, and post processing. It has been shown that the elongation flow plays an important role in CNT alignment.[21,79] The shear and capillary forces involved can transform the polydomain nematic solution into a single-domain, highly oriented fiber. The fiber can be dried when the solvent evaporates away. The CNT fibers spun with diethyl ether exhibit a collapsed structure with lots of voids, while CNT fibers spun with water or ethanol show a uniform circular cross section. These results show that decreasing evaporation of the solvent allows sufficient time to anneal the fiber structure with fewer internal voids.

The importance of the liquid-crystalline spinning technique of CNT fibers is parallel to that of the polymers, such as Kevlar and Zylon. However, the technique development is still in its infancy. Further optimization of the dispersion, spinning conditions, coagulation conditions, and post treatment are expected to improve the physical properties of the fibers. For example, annealing the CNT fibers at 1400 K in argon for 24 h resulted in an order of magnitude increase in electrical conductivity as compared to the tubes annealed at 300 K.[76] The tensile strength and Young's modulus of the CNT fibers after heat treatment at 2000 K could be enhanced six times and twice, respectively, due to the welding effect at the nanotube joints.[73,75] The hot drawing during the post processing has been reported to significantly improve the CNT alignment and therefore enhance the tensile strength and Young's modulus.[80,81] For polymeric fibers and pitch-based carbon fibers with ultrahigh orientation, Young's modulus values close to 70% and 90% of the theoretical modulus have been achieved, respectively.[19,82] Therefore, future work on efficiently controlling nanotube alignment in the CNT fibers is very necessary. In addition, CNTs with monodisperse diameter and absence of catalyst particles are desirable to achieve high-tensile-strength fibers.[83]

Higher-molecular-weight polymers result in higher-tensile-strength fibers.[84,85] Similarly, longer CNTs increase intertube contact length, which is crucial to enhance tube-to-tube load transfer. A recent report on the CNT fibers from millimeter-long nanotubes has given a tensile strength as high as 8.8 GPa.[72] Developments of strategies on synthesizing ultralong CNTs have been reported. For example, half-centimeter-long CNT arrays have been synthesized by adding a small amount of water into the standard CVD environment.[86,87] Another factor that affects the mechanical properties of CNT fibers is the CNT diameter of inner and outer parts. The large ratio tends to induce CNTs to collapse. Collapsed CNTs maximize the contact area and enhance tube-to-tube load transfer, resulting in improved tensile strength of the CNT fibers. A recent report on the CNT fibers made from dog-bone-shaped nanotubes has shown such an improvement.[71,72] Centimeter-long collapsed nanotubes without the presence of catalyst particles are expected to yield the CNT fiber tensile strength that approaches the theoretical value.

5.2. Thin Films

CNTs have been proposed for high-performance thin-film electronic applications because of their potentially high charge-carrier mobilities and large current-carrying capacities. Semiconducting CNTs work as transistors while metallic CNTs act as electrical conductors. The film surface density and the CNT alignment are considered as critical elements for fabricating high-performance CNT-based thin-film electronic devices.

Liquid-crystalline processing has been recognized as a promising route to fabricate highly dense, highly aligned CNT thin films for electronic devices.[13] Among various strategies to make liquid-crystal phases of CNTs, drop drying is a simple and straightforward method. Millimeter-scale monolayer CNT thin films have been reported via drop drying.[13] The resulting oriented CNT thin films can be used to fabricate CNT-based thin-film transistors (TFTs; Figure 12). The reported oriented CNT-based TFT performance is even better than that of the orientated silicon-based TFT.[13]

It should be noted that the device performance and electrical characteristics of aligned CNT-based TFTs processed via the liquid-crystalline phase are very high compared to those reported for rather complicated CNT-based TFTs. The simple and easy fabrication of liquid-crystalline processing of CNTs is very promising towards the practical application of low-cost, large-scale, high-performance CNT-based electronic devices. If the effective separation of metallic and semiconducting CNTs could be developed, unique electrical properties of individual CNTs would be fully utilized in thin-film microdevices using liquid-crystalline processing.

6. Summary and Outlook

We have described recent developments of CNTs as liquid crystals, covering rigid-rod steric theory, liquid-crystal fabrication, solution properties, and processing techniques. With the remarkable progress in research on CNTs over past seventeen years, nanotubes as liquid-crystal materials become more and more important. Control of nanotube alignment has been recognized to play a crucial role in developing the practical techniques in the exploitation of individual nanotube properties in the macroscopic assemblies. The intrinsic self-assembling nature in the liquid-crystalline phase is promising in achieving such macroscopic nanotube alignment. As the liquid crystals are highly sensitive to the external forces, the applied fields, such as mechanical shear flow, electric or magnetic stimuli, as well as surface tension, could significantly improve the nanotube alignment in the liquid-crystalline phase.

Understanding dynamic interactions between the disclinations in the CNT system is very important to control the nanotube alignment. In liquid-crystal science, the pairwise interaction of disclinations is analogous to the electrostatic interaction between the line charges.[1,2] Disclinations of opposite sign attract and annihilate each other, while disclinations of the same sign repel each other. This interaction results in the annihilation of defects and therefore a decrease in their number density. However, the details of these

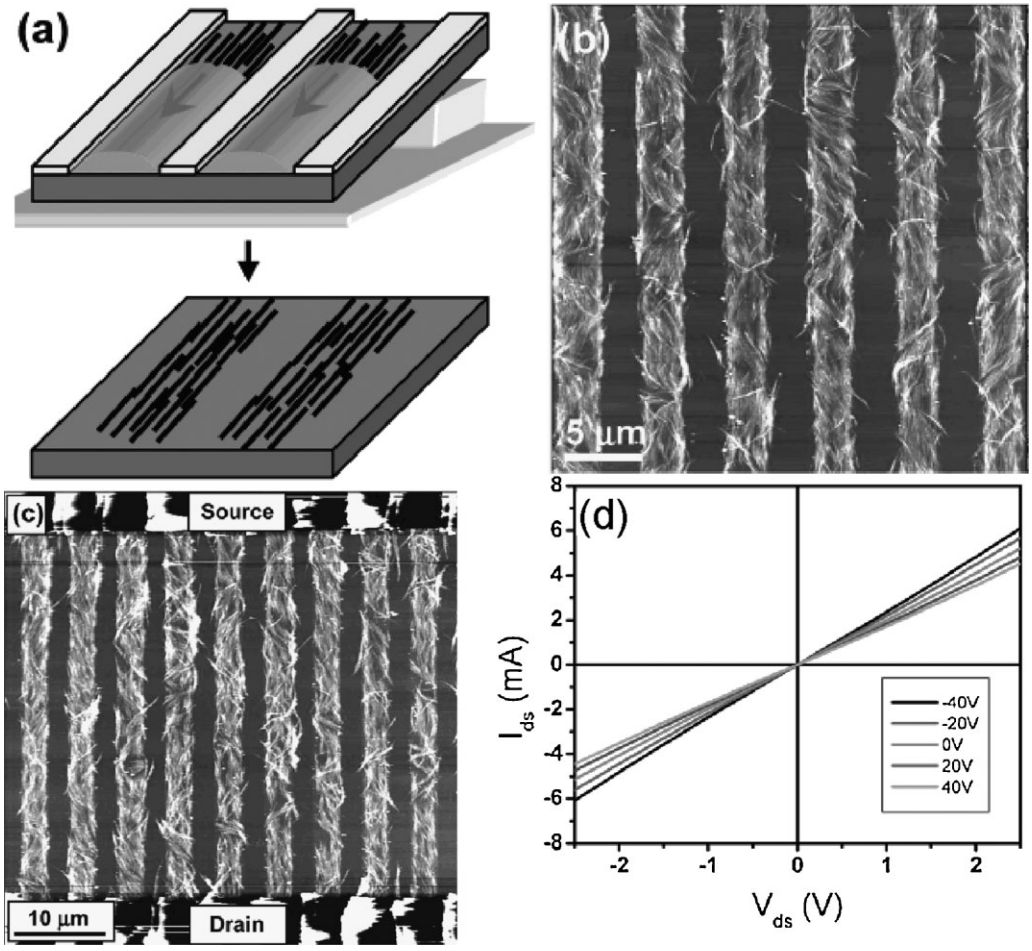

Figure 12. a) Schematic image of liquid-crystalline fabrication of a SWNT thin film, b) AFM height image of SWNT films showing uniaxially oriented, densely packed SWNT bundles, c) AFM height image of a SWNT-TFT device of backgated-oriented SWNTs with Au source/drain electrodes, and d) output characteristics of device shown in (c) when the gate voltage is swept from −40 to 40 V. Adapted from Reference [13]. Copyright 2006, American Chemistry Society.

processes are still far from being understood due to both the complexity of potential many-body disclination interactions and the lack of suitable, high-resolution, experimental methods. Nanotube liquid crystals will be a model system to study such physical issues. Based on the nanotube orientation, the director fields can be directly mapped. Thus, disclination interactions at the nanosclae can be investigated.

Nanotubes have been considered to be an excellent reinforcing agent for polymer nanocomposites.[88,89] CNTs act as an orientation template and nucleating agent for polymer crystallization.[22,90–92] However, the critical challenge in nanotube-reinforced polymer composites lies in uniform dispersion, nanotube alignment, strong nanotube-matrix adhesion, nanotube length, and nanotube loading. [93,94] To achieve high nanotube loading with good orientation in a polymer matrix has been a challenge.[88,89,93,94] A possible solution to this difficulty is to use oriented nanotube fiber or film in which the nanotubes are already well aligned.[95] In this well-aligned fiber or film, the monomer can be infiltrated followed by in situ polymerization. Another method is to infiltrate the polymer solution into the nanotube fibers with subsequent crystallization if the polymer is semicrystalline. Resulting nanotube-fiber-based polymer nanocomposites will have potential applications in high-performance structural materials,[88,89] muscle-like actuators,[96] and energy-harvesting devices.[97]

As liquid-crystal materials are starting to be used in biomedical applications such as biosensors, biology imaging, artificial muscles, gene delivery, and so on;[48,49] CNT liquid crystals may also have potential applications in biological systems. Recent studies have shown that functionalized nanotubes and nitrogen-doped nanotubes can be more biocompatible and less toxic than pristine nanotubes.[98,99] One possible application is that nanotube liquid crystals may be useful as novel responsive fluids. For example, study of the nanotube liquid-crystal orientation depending on the interaction with analyte solutions containing specific biomolecules could be very interesting, as it offers possibilities for use in biosensor applications.[100] Due to excellent mechanical properties, nanotubes are suitable as bone-scaffold material. It has been reported that osteoblasts, the bone-forming cells, can grow on the nanotube aggregates and the cultured bone cells can further produce mineralized hydroxyapatite (HA) nanocrystals.[101] Nanotube fibers through the liquid-crystal route will provide anisotropic scaffolds for bone regeneration as well as permanent mechanical support of the damaged bone tissue.

Acknowledgements

We thank Professors M. Pasquali and A. Griffin for critical comments. Financial support from Air Force Office of Scientific Research is acknowledged.

[1] P. G. de Gennes, P. Prost, *The Physics of Liquid Crystals*, Clarendon Press, Oxford, UK **1993**.
[2] M. Kleman, Points, *Lines and Walls: in Liquid Crystals, Magnetic Systems, and Various Ordered Media*, Wiley, Chichester, UK **1983**.
[3] F. C. Frank, *Discuss. Faraday Soc.* **1958**, *25*, 19.
[4] a) S. J. Zhang, E. M. Terentjev, A. M. Donald, *Macromolecules* **2004**, *37*, 390; b) S. J. Zhang, E. M. Terentjev, A. M. Donald, *Langmuir* **2005**, *21*, 3539; c) S. J. Zhang, E. M. Terentjev, A. M. Donald, *J. Phys. Chem. B* **2005**, *109*, 13195; d) S. J. Zhang, E. M. Terentjev, A. M. Donald, *Macromol. Rapid Commun.* **2005**, *26*, 911; e) S. J. Zhang, E. M. Terentjev, A. M. Donald, *Eur. Phy. J. E* **2003**, *11*, 367.
[5] P. E. Cladis, W. Van Saarloos, P. L. Finn, A. R. Kortan, *Phys. Rev. Lett.* **1987**, *58*, 222.
[6] M. S. P. Shaffer, A. H. Windle, *Macromolecules* **1999**, *32*, 6864.
[7] W. H. Song, I. A. Kinloch, A. H. Windle, *Science* **2003**, *302*, 1363.
[8] W. H. Song, A. H. Windle, *Macromolecules* **2005**, *38*, 6181.
[9] V. A. Davis, L. E. Ericson, A. Nicholas, G. Parra-Vasquez, H. Fan, Y. Wang, V. Prieto, J. A. Longoria, S. Ramesh, R. K. Saini, C. Kittrell, W. E. Billups, W. W. Adams, R. H. Hauge, R. E. Smalley, M. Pasquali, *Macromolecules* **2004**, *37*, 154.
[10] P. K. Rai, R. A. Pinnick, A. Nicholas, G. Parra-Vasquez, V. A. Davis, H. K. Schmidt, R. H. Hauge, R. E. Smalley, M. Pasquali, *J. Am. Chem. Soc.* **2006**, *128*, 591.
[11] S. D. Bergin, V. Nicolosi, S. Giordani, A. de Gromard, L. Carpenter, W. J. Blau, J. N. Coleman, *Nanotechnology*, **2007**, *18*, 455705.
[12] Q. W. Li, Y. T. Zhu, I. A. Kinloch, A. H. Windle, *J. Phys. Chem. B* **2006**, *110*, 13962.
[13] K. Ko, V. V. Tsukruk, *Nano Lett.* **2006**, *6*, 1443.
[14] R. Duggal, F. Hussain, M. Pasquali, *Adv. Mater.* **2006**, *18*, 29.
[15] S. Badaire, C. Zakri, M. Maugey, A. Derre, J. N. Barisci, G. Wallace, P. Poulin, *Adv. Mater.* **2005**, *17*, 1673.
[16] a) C. Zakri, P. Poulin, *J. Mater. Chem.* **2006**, *16*, 4095; b) S. E. Moulton, M. Maugey, P. Poulin, G. G. Wallace, *J. Am. Chem. Soc.* **2007**, *129*, 9452.
[17] E. K. Hobbie, D. J. Fry, *Phys. Rev. Lett.* **2006**, *97*, 036101.
[18] C. Zakri, *Liq. Cryst. Today* **2007**, *16*, 1.
[19] H. G. Chae, S. Kumar, *J. Appl. Poly. Sci.* **2006**, *100*, 791.
[20] L. M. Ericson, H. Fan, H. Peng, V. A. Davis, W. Zhou, J. Sulpizio, Y. Wang, R. Booker, J. Vavro, C. Guthy, A. N. G. Para-Vasquez, M. J. Kim, S. Ramesh, R. K. Saini, C. Kittrell, G. Lavin, H. Schmidt, W. W. Adams, W. E. Billups, M. Pasquali, W. F. Hwang, R. H. Hauge, J. E. Fischer, R. E. Smalley, *Science* **2004**, *305*, 1447.
[21] S. J. Zhang, K. K. K. Koziol, I. A. Kinloch, A. H. Windle, *Small* **2008**, *4*, 217.
[22] S. J. Zhang, M. L. Minus, L. B. Zhu, C. P. Wong, S. Kumar, *Polymer* **2008**, *49*, 1356.
[23] L. Onsager, *Ann. N. Y. Acad. Sci.* **1949**, *56*, 627.
[24] P. J. Flory, *Proc. R. Soc. London Ser. A* **1956**, *234*, 73.
[25] A. M. Donald, A. H. Windle, *Liquid-Crystalline Polymers*, Cambridge University Press, Cambridge, UK **1992**.
[26] Y. Sabba, E. L. Thomas, *Macromolecules* **2004**, *37*, 4815.
[27] A. M. Somoza, C. Sagui, C. Roland, *Phys. Rev. B* **2001**, *63*, 081403.
[28] R. J. Bushby, O. R. Lozman, *Curr. Opin Colloid Interface Sci.* **2002**, *7*, 343.
[29] Y. K. Kwon, D. Tomanek, *Phys. Rev. Lett.* **2000**, *84*, 1483.
[30] a) J. Liu, A. G. Rinzler, H. Dai, J. H. Hafner, R. K. Bradley, P. J. Boul, A. Lu, T. Iverson, K. Shelimov, C. B. Huffman, F. Rodriguez-Macias, Y. S. Shon, T. R. Lee, D. T. Collert, R. E. Smalley, *Science* **1998**, *280*, 1253; b) A. Kuznetsova, D. B. Mawhinney, V. Naumenko, J. T. Yates, Jr, J. Liu, R. E. Smalley, H. H. Hwu, J. G. Chen, *J. Am. Chem. Soc.* **2001**, *123*, 10699; c) J. Zhang, H. Zou, Q. Qing, Y. Yang, Q. Li, Z. Liu, X. Guo, Z. Du, *J. Phys. Chem. B* **2003**, *107*, 3712; d) Q. W. Li, H. Yan, Y. C. Ye, J. Zhang, Z. F. Liu, *J. Phys. Chem. B* **2002**, *106*, 11085.
[31] S. Niyogi, M. A. Hamon, H. Hu, B. Zhao, P. Bhowmik, R. Sen, M. E. Itkis, R. C. Haddon, *Acc. Chem. Res.* **2002**, *35*, 1105.
[32] K. Esumi, A. Ishigami, A. Nakajima, K. Sawada, H. Honda, *Carbon* **1996**, *34*, 279.
[33] M. S. P. Shaffer, K. Koziol, *Chem. Commun.* **2002**, 2074.
[34] S. L. Kwolek, P. W. Morgan, J. R. Schaefgen, L. W. Gulrich, *Macromolecules*, **1977**, *10*, 1390.
[35] R. Bair, P. W. Morgan, J. L. Killian, *Macromolecules*, **1977**, *10*, 1396.
[36] S. J. Zhang, I. A. Kinloch, A. H. Windle, *Nano Lett.* **2006**, *6*, 568.
[37] S. J. Zhang, E. M. Terentjev, A. M. Donald, *Liq. Cryst.* **2005**, *32*, 69.
[38] S. D. Hudson, J. W. Fleming, E. Gholz, E. L. Thomas, *Macromolecules*, **1993**, *26*, 1270.
[39] W. Zhou, P. A. Heiney, H. Fan, R. E. Smalley, J. E. Fishcer, *J. Am. Chem. Soc.* **2005**, *127*, 1640.
[40] W. Zhou, J. E. Fischer, P. A. Heiney, H. Fan, V. A. Davis, M. Pasquali, R. E. Smalley, *Phys. Rev. B* **2005**, *72*, 045440.
[41] S. Ramesh, L. M. Ericson, V. A. Davis, R. K. Sain, C. Kittrell, M. Pasquali, W. E. Billups, W. W. Adam, R. H. Hauge, R. E. Smalley, *J. Phys. Chem. B* **2004**, *108*, 8794.
[42] A. B. Dalton, C. Stephan, J. N. Coleman, B. McCarthy, P. M. Ajayan, S. Lefrant, P. Bernier, W. J. Blau, H. J. Byrne, *J. Phys. Chem. B* **2000**, *104*, 10012.
[43] R. Shvartzman-Cohen, Y. Levi-Kalisman, E. Nativ-Roth, R. Yerushalmi-Rozen, *Langmuir* **2004**, *20*, 6085.
[44] V. A. Sinani, M. K. Gheith, A. A. Yaroslavov, A. A. Rakhnyanskays, K. Sun, A. A. Mamedov, J. P. Wicksted, N. A. Kotov, *J. Am. Chem. Soc.* **2005**, *127*, 3463.
[45] T. Takahashi, K. Tsunoda, H. yajima, T. Ishii, *Jpn. J. Appl. Phys.* **2004**, *43*, 3636.
[46] M. J. O'Connell, P. Boul, L. M. Ericson, C. Huffman, Y. Wang, E. Haroz, C. Kuper, J. Tour, K. D. Ausman, R. E. Smalley, *Chem. Phys. Lett.* **2001**, *342*, 265.
[47] G. T. Stewart, *Liq. Cryst.* **2004**, *31*, 443.
[48] S. J. Woltman, G. D. Jay, G. P. Crawford, *Nat. Mater.* **2007**, *6*, 929.
[49] P. Palffy-Muhoray, *Phys. Today* **2007**, *60*, 54.
[50] R. D. Deegan, O. Bakajin, T. F. Dupont, G. Huber, S. R. Nagel, T. A. Witten, *Nature* **1997**, *389*, 827.
[51] W. Wang, G. Lieser, G. Wegner, *Liq. Cryst.* **1993**, *15*, 1.
[52] L. S. Li, A. P. Alivisatos, *Adv. Mater.* **2003**, *15*, 408.
[53] I. I. Smalyukh, O. Zribi, J. Butler, O. D. Lavrentovich, G. C. L. Wong, *Phys. Rev. Lett.* **2006**, *96*, 177801.
[54] V. C. Moore, M. S. Strano, E. H. Haroz, R. H. Hauge, R. E. Smalley, *Nano Lett.* **2003**, *3*, 1379.
[55] L. Huang, X. Cui, G. Dukovic, S. P. O'Brien, *Nanotechology* **2004**, *15*, 1450.
[56] M. F. Islam, A. M. Alsayed, Z. Dogic, J. Zhang, T. C. Lubensky, A. G. Yodh, *Phys. Rev. Lett.* **2004**, *92*, 0883031.
[57] M. F. Islam, M. Nobili, F. Ye, T. C. Lubensky, A. G. Yodh, *Phys. Rev. Lett.* **2005**, *95*, 1483011.
[58] S. S. Rahatekar, K. K. K. Koziol, S. A. Butler, J. A. Elliott, M. S. P. Shaffer, M. R. Mackley, A. H. Windle, *J. Rheogoly* **2006**, *50*, 599.
[59] I. A. Kinloch, S. A. Roberts, A. H. Windle, *Polymer* **2002**, *43*, 7483.
[60] M. Doi, S. F. Edwards, *The Theory of Polymer Dynamics*, Oxford University Press, New York **1986**.
[61] G. G. Fuller, *Optical Rheometry of Complex Fluids*, Oxford University Press, New York **1995**.

[62] Y. Y. Huang, S. V. Ahir, E. M. Terentjev, *Phys. Rev. B* **2006**, *73*, 125422.
[63] E. K. Hobbie, *Phys. Rev. E* **2007**, *75*, 012501.
[64] M. M. Denn, *Annu. Rev. Fluid Mech.* **2001**, *33*, 265.
[65] a) S. B. Kharchenko, J. F. Douglas, J. Obrzut, E. A. Grulke, K. B. Migler, *Nat. Mater.* **2004**, *3*, 564; b) M. Pasquali, *Nat. Mater.* **2004**, *3*, 509.
[66] G. Conio, E. Bianchi, A. Ciferri, W. R. Krigbaum, *Macromolecules* **1984**, *17*, 856.
[67] S. M. Aharoni, E. K. Walsh, *Macromolecules* **1979**, *12*, 271.
[68] D. Fry, B. Langhorst, H. Kim, E. Grulke, H. Wang, E. K. Kobbie, *Phys. Rev. Lett.* **2005**, *95*, 0383041.
[69] Y. L. Li, I. A. Kinloch, A. H. Windle, *Science* **2004**, *304*, 276.
[70] M. Motta, Y. L. Li, I. A. Kinloch, A. H. Windle, *Nano Lett.* **2005**, *5*, 1529.
[71] M. Motta, A. Moisala, I. A. Kinloch, A. H. Windle, *Adv. Mater.* **2007**, *19*, 3721.
[72] K. Koziol, J. Vilatela, A. Moisala, M. Motta, P. Cunniff, M. Sennett, A. Windle, *Science* **2007**, *318*, 1892.
[73] K. L. Jiang, Q. Q. Li, S. S. Fan, *Nature* **2002**, *419*, 801.
[74] M. Zhang, K. R. Atkinson, R. H. Baughman, *Science* **2004**, *306*, 1358.
[75] X. B. Zhang, K. L. Feng, P. Liu, L. Zhang, J. Kong, T. H. Zhang, Q. Q. Li, S. S. Fan, *Adv. Mater.* **2006**, *18*, 1505.
[76] X. F. Zhang, Q. W. Li, Y. Tu, Y. Li, Y. Coulter, L. Zheng, Y. Zhao, Q. Jia, D. E. Peterson, Y. T. Zhu, *Small*, **2007**, *3*, 244.
[77] S. J. Zhang, L. B. Zhu, M. L. Minus, H. G. Chae, S. Jagannathan, C. P. Wong, J. Kowalik, L. B. Roberson, S. Kumar, *J. Mater. Sci.* **2008**, *43*, 4356.
[78] T. Liu, S. Kumar, *Nano Lett.* **2003**, *3*, 647.
[79] W. Zhou, J. Vavro, C. Guthy, K. I. Winey, J. E. Fischer, L. M. Ericson, S. Ramesh, R. Saini, V. A. Davis, C. Kittrell, M. Pasquali, R. H. Hauge, R. E. Smalley, *J. Appl. Phys.* **2004**, *95*, 649.
[80] B. Vigolo, P. Poulin, M. Lucas, P. Launois, P. Bernier, *Appl. Phys. Lett.* **2002**, *81*, 1210.
[81] P. Miaudet, S. Badaire, M. Maugey, A. Derre, V. Pichot, P. Launois, P. Poulin, C. Zakri, *Nano Lett.* **2005**, *5*, 2212.
[82] M. L. Minus, S. Kumar, *JOM*, **2005**, *57*, 52.
[83] H. G. Chae, S. Kumar, *Science* **2008**, *319*, 908.
[84] I. M. Ward, P. D. Coates, M. M. Dumoulin, *Solid Phase Processing of Polymers*, Hanser Gerdner, Germany **2000**.
[85] L. M. Nicholson, K. S. Whitley, T. S. Gates, J. A. Hinkley, *J. Mater. Sci.* **2000**, *35*, 6111.
[86] Q. W. Li, X. F. Zhang, R. F. DePaula, L. X. Zheng, Y. H. Zhao, L. Stan, T. G. Holesinger, P. N. Arendt, D. E. Peterson, Y. T. Zhu, *Adv. Mater.* **2006**, *18*, 3160.
[87] Y. Yun, V. Shanov, Y. Tu, S. Subramaniam, M. J. Schulz, *J. Phys. Chem. B* **2006**, *110*, 23920.
[88] R. H. Baughman, A. A. Zakhidov, W. A. de Heer, *Science* **2002**, *297*, 787.
[89] H. G. Chae, M. L. Minus, A. Rasheed, S. Kumar, *Polymer* **2007**, *48*, 3781.
[90] a) M. L. Minus, H. G. Hae, S. Kumar, *Polymer* **2006**, *47*, 3705; b) H. G. Chae, M. L. Minus, S. Kumar, *Polymer* **2006**, *47*, 3494.
[91] L. Li, C. Y. Li, C. Ni, *J. Am. Chem. Soc.* **2006**, *128*, 1692.
[92] S. J. Zhang, S. Kumar, *Macromol. Rapid Commun.* **2008**, *29*, 557.
[93] J. N. Coleman, U. Khan, Y. K. Gun'ko, *Adv. Mater.* **2006**, *18*, 689.
[94] R. Andrews, D. Jacques, D. L. Qian, T. Rantell, *Acc. Chem. Res.* **2002**, *35*, 1008.
[95] H. S. Peng, *J. Am. Chem. Soc.* **2008**, *130*, 42.
[96] a) S. V. Ahir, A. M. Squires, A. R. Tajbakhsh, E. M. Terentjev, *Phys. Rev. B* **2006**, *73*, 085420; b) S. Courty, J. Mine, A. R. Tajbakhsh, E. M. Terentjev, *Europhys. Lett.* **2003**, *64*, 654; c) S. V. Ahir, E. M. Terentjev, *Nat. Mater.* **2005**, *4*, 491; d) S. Lu, S. V. Ahir, E. M. Terentjev, B. Panchapakesan, *Appl. Phys. Lett.* **2007**, *91*, 103106; e) V. H. Ebron, Z. Yang, D. J. Seyer, M. E. Kozlov, J. Oh, H. Xie, J. Razal, L. J. Hall, J. P. Ferraris, A. G. MacDiamid, R. H. Baughman, *Science* **2006**, *311*, 1580; f) T. Mirfakhrai, J. D. W. Madden, R. H. Baughman, *Mater. Today* **2007**, *10*, 30; g) R. H. Baughman, C. X. Cui, A. A. Zakhidov, Z. Iqbal, J. N. Barisci, G. M. Spinks, G. G. Wallace, A. Mazzoldi, D. D. Rossi, A. G. Rinzler, O. Jaschinski, S. Roth, M. Kertesz, *Science* **1999**, *284*, 1340.
[97] a) V. Sgobba, D. M. Guldi, *J. Mater. Chem.* **2008**, *18*, 153; b) R. Ulbricht, S. B. Lee, X. Jiang, K. Inoue, M. Zhang, S. Fang, R. H. Baughman, *Sol. Energy Mater. Sol. Cells* **2007**, *91*, 416; c) J. D. W. Madden, J. N. Barisci, P. A. Anquetil, G. M. Spinks, G. G. Wallace, R. H. Baughman, I. W. Hunter, *Adv. Mater.* **2006**, *18*, 870.
[98] J. C. Carrero-Sanchez, A. L. Elias, R. Mancilla, G. Arrellin, H. Terrones, J. P. Laclette, M. Terrones, *Nano Lett.* **2006**, *6*, 1609.
[99] a) Z. Liu, X. M. Sun, N. Nakayama-Ratchford, H. J. Dai, *ACS Nano* **2007**, *1*, 50; b) N. W. S. Kam, M. O'Connell, J. A. Wisdom, H. J. Dai, *PNAS* **2005**, *102*, 11600.
[100] a) S. L. Helfinstine, O. D. lavrentovich, C. J. Woolverton, *Lett. Appl. Microbio.* **2006**, *43*, 27; b) Y. A. Nastishin, H. Liu, T. Schneider, V. Nazarenko, R. Vasyuta, S. V. Shiyanovskii, O. D. Lavrentovich, *Phys. Rev. E* **2005**, *72*, 041711; c) S. V. Shiyanovskii, O. D. Lavrentovich, T. Schneider, T. Ishikawa, I. I. Smalyukh, C. J. Woolverton, G. D. Niehaus, K. J. Doane, *Mol. Cryst. Liq. Cryst.* **2005**, *434*, 587.
[101] a) L. P. Zanello, B. Zhao, H. Hu, R. C. Haddon, *Nano Lett.* **2006**, *6*, 562; b) Y. Usui, K. Aoki, N. Narita, N. Murakami, I. Nakamura, K. Nakamura, N. Ishigaki, H. Yamazaki, H. Horiuchi, H. Kato, S. Taruta, Y. A. Kim, M. Endo, N. Saito, *Small* **2008**, *4*, 240.

Received: February 1, 2007
Revised: February 12, 2008

